**J Neurosurg (Spine 2) 99:**206–213, 2003

# Tethering of the spinal cord in mouse fetuses and neonates with spina bifida

**DOROTHEA STIEFEL, M.D., TAKASHI SHIBATA, M.D., MARTIN MEULI, M.D., PATRICK G. DUFFY, M.D., AND ANDREW J. COPP, M.D., PH.D.**

*Neural Development Unit, Institute of Child Health, University College London; Department of Paediatric Urology, Great Ormond Street Hospital for Children NHS Trust, London, United Kingdom; Department of Pediatric Surgery, University Children's Hospital Zurich, Switzerland; and Department of Urology, Hokkaido University, Sapporo, Japan*

*Object.* Tethering of the spinal cord is a well-known complication in humans with spina bifida aperta or occulta. Its pathogenesis consists of a pathological fixation of the spinal cord resulting in traction on the neural tissue which, in turn, leads to ischemia and progressive neurological deterioration. Although well established in humans, this phenomenon has not been described in animal models of spina bifida.

*Methods.* A fetal mouse model with naturally occurring, genetically determined spina bifida was produced by generating double mutants between the curly tail and loop-tail mutant strains. Microdissection, labeling with 1,1′-dioctadecyl-3,3,3,′,3′-tetramethylindocarbocyanine perchlorate, immunohistochemistry for neurofilaments, H & E staining of histological sections, and whole-mount skeletal preparations were performed and comparisons made among mutant and normal fetuses.

Normal fetuses exhibited the onset of progressive physiological ascent of the spinal cord from embryonic Day 15.5. Spinal cord ascent resulted, by embryonic Day 18.5, in spinal nerve roots that pass caudolaterally from the spinal cord toward the periphery. In contrast, fetuses with spina bifida exhibited spinal cord tethering that resulted, at embryonic Day 18.5, in nerve roots that run in a craniolateral direction from the spinal cord. The region of closed spinal cord immediately cranial to the spina bifida lesion exhibited marked narrowing, late in gestation, suggesting that a potentially damaging stretch force is applied to the spinal cord by the tethered spina bifida lesion.

*Conclusions.* This mouse model provides an opportunity to study the onset and early sequelae of spinal cord tethering in spina bifida.

**KEY WORDS • neural tube • myelomeningocele • embryo • tethered cord • spina bifida • mouse**

PHYSIOLOGICAL ascent of the spinal cord begins after gestational Day 54 in the human embryo, with the conus medullaris reaching the level of L1–3 by 3 months postpartum.[9,13] Following this stage, the presence of a conus medullaris below L-3 is suggestive of low fixation of the spinal cord, which may be symptomatic in the so-called TCS.

Spinal cord tethering is characterized by progressively intense symptoms such as back pain due to scoliosis; incontinence resulting from a neurogenic bladder; and numbness, weakness, or pain of the lower extremity and foot deformity due to progressive sensory and motor deficit.[3,6,14–16,22–25,29,34] Spinal cord tethering has been described mostly in children and adolescents,[4,6,14,15,18,22–24,32–34] particularly in those with spinal dysraphism (spina bifida aperta or occulta). Cutaneous stigmata, such as dimples, hairy patches, abnormal pigmentation and lipomas, are often found at the site of the spinal abnormality.[15–17,24,29,30,32] Spinal cord tethering, however, may also occur in patients without cutaneous signs, thus presenting a truly occult spinal dysraphism.[20,29]

The various conditions leading to spinal cord tethering include a thickened or tight terminal filum, abnormalities of the conus medullaris such as syringomyelia, diplomyelia, diastematomyelia, dermoids or intradural cysts,[5,14,15,24,29,30,33] and the various forms of spina bifida aperta or occulta. Even though the origin of spinal cord tethering can be variable, its pathogenesis appears more uniform, involving pathological fixation of the spinal cord in an abnormal (usually caudal) position.[3,24,26,29,30,33] This provokes traction with daily body movements, leading to repeated extension and distortion of the spinal cord and, finally, to ischemia, progressive neurological deterioration, and even skeletal deformity.[24]

The aim of our study was to investigate the ascent of the spinal cord in the fetal mouse; to our knowledge, neither

*Abbreviations used in this paper:* DiI = 1,1′-dioctadecyl-3,3,3,′,3′-tetramethylindocarbocyanine perchlorate; FCS = fetal calf serum; IgG = immunoglobulin G; PBS = phosphate-buffered saline; PFA = paraformaldehyde; PTX = PBS combined with 1% triton X-100; TBS = Tris-buffered saline; TCS = tethered cord syndrome.

fetal ascent nor tethering of the spinal cord has been documented in a suitable animal model. We chose a mouse model with naturally occurring spina bifida, enabling a comparison between fetuses and neonates with and without spina bifida. We determined the time of onset of the spinal cord ascent and documented findings of tethering and its early sequelae. In particular, we describe a compensational stretching mechanism of the closed part of the spinal cord in spina bifida animals, as a consequence of the tethering of the open spinal lesion.

## Materials and Methods

*Mouse Strains*

The loop-tail mutation is an autosomal-recessive cause of severe neural tube closure defects (craniorachischisis) with heterozygote effects including occasional spina bifida and tail flexion defects.[27] The curly tail mutation is an autosomal-recessive, partially penetrant, cause of mouse spina bifida.[12] Mice harboring both loop-tail and curly tail mutations have severe spina bifida in almost all cases (Pavlovska and Copp, unpublished data).

*Collection of Fetuses and Newborns*

Mice were maintained on a 12-hour light, 12-hour dark cycle (lights on from 7:00 am–7:00 pm). Overnight matings between doubly heterozygous loop-tail/curly tail males and homozygous curly tail female mice were checked for vaginal plugs the following morning; the day on which a copulation plug was found was designated embryonic Day 0.5. Litters were collected at intervals between embryonic Days 11.5 and 18.5, as well as on postnatal Day 1. Features in animals with spina bifida were compared with those in their phenotypically normal littermates. Pregnant females were killed by cervical dislocation, and fetuses were dissected in Dulbecco modified Eagle medium containing 10% FCS. The extraembryonic membranes were removed. The fetuses were rinsed in PBS and then placed on a frozen metal plate before fixation. Newborn pups were killed by an overdose (10 ml/kg body weight) of midazolam mixed 1:1 with fentanyl and diluted to 50% in distilled water. All experiments with mice were performed with appropriate licensing under the Animals (Scientific Procedures) Act, 1986 of the United Kingdom government.

*General Morphology*

Fetuses obtained between embryonic Days 13.5 and 18.5 as well as postnatal Day 1 pups (35 total; two–four of each phenotype at each age) were fixed in Bouin solution for 2 to 7 days, depending on age. After serial dehydration, they were embedded in paraffin wax and sectioned transversely at 8-μm thickness. Sections were dewaxed, serially rehydrated to distilled water, stained with Ehrlich H & E for 10 and 5 minutes, respectively, dehydrated, and mounted in DPX. Photomicrographs (for all specimens) were obtained using color reversal film on light microscopes.

*Microdissection Procedure*

After posterior laminectomy, embryonic Day 18.5 fetuses (two with spina bifida and two controls) were placed supine, and the vertebral bodies were removed to separate the spinal cord from the vertebral column. This procedure enabled visualization of the intact posterior root ganglia and the spinal cord with its spinal nerve roots, especially the portion of the sensory roots connecting the posterior root ganglia with the spinal cord.

*Labeling With DiI*

After laminectomy, the posterior root ganglia and their respective spinal nerve roots at L-6 and S-1 were identified in the embryonic Day 18.5 fetuses (three with spina bifida and three control fetuses). To visualize the sensory nerve roots between the posterior root ganglia and the posterior sensory horn, crystals of DiI, a substance with an exclusively lipophilic character, were dissolved in 2.5 mg/ml dimethylformamide prior to injection into the L-6 and S-1 posterior root ganglia by using a fine glass needle connected to an air pump. After injection, specimens were fixed at 4˚C overnight in 4% paraformaldehyde in PBS (4% PFA), followed by incubation at 37˚C for 2 to 3 weeks to allow the diffusion of DiI from the injection site along the axons.

*Immunohistochemical Analysis*

Fetuses obtained on embryonic Days 12.5 to 18.5 as well as postnatal Day 1 pups (27 total; one–three of each phenotype at each age) were fixed in 4% PFA for 2 to 7 days, depending on age. They were dehydrated through an ethanol series and embedded in paraffin wax. Sections were cut at 8-μm thickness in a parasagittal plane, dewaxed, rehydrated, and unmasked with Declere (Cell Marque, Hot Springs, AK) in a microwave oven. Endogenous peroxidase was quenched by incubation in 0.6% $H_2O_2$ in TBS (0.05 M Tris, 0.15 M NaCl, pH 7.6) for 7.5 minutes and nonspecific epitopes were blocked by exposure to 10% FCS in 0.5% Triton X-100 in TBS. Monoclonal antineurofilament 68 antibody (N5139, mouse $IgG_1$; Sigma Chemical Co., St. Louis, MO) was applied overnight at 4˚C, diluted 1:400 in TBS containing 1% FCS and 0.5% Triton X-100. The following day the sections were washed in TBS/1% FCS/0.5% Triton X-100 and then exposed for 1 hour to secondary biotinylated rabbit anti–mouse IgG antibody (DAKO Corp., Carpinteria, CA), diluted 1:500 in the same solution. Several washes in TBS were followed by reaction with streptavidin–biotinylated horseradish peroxidase (DAKO Corp.) for 30 minutes at room temperature. Coloration of the neurofilaments was produced using 3,3′-diaminobenzidine (Sigma). Control sections, in which the primary antibody was replaced by 1% FCS/TBS, were negative in all cases.

*Immunohistochemical Analysis of Whole-Mount Preparations*

Fetuses obtained on embryonic Days 13.5 to 18.5 (28 fetuses; one–three of each phenotype at each age) were eviscerated, and those older than 15.5 days of gestation were also deskinned. After fixation in 4% PFA for at least 48 hours, fetuses were bleached in 6% $H_2O_2$ in PTX for 30 minutes to 2 hours, depending on age. After several washes in PTX, fetuses were incubated for 3 to 5 hours in a blocking buffer solution (1 mg/ml bovine serum albumin, 5% heat-inactivated sheep serum in PTX) to quench endogenous peroxidase and to block nonspecific epitopes. Monoclonal antineurofilament 68 antibody was added to the solution, diluted 1:100, incubation was continued for 7 to 10 days at 4˚C on a rocking plate, and followed by washes in PTX for 2 days. The secondary biotinylated rabbit anti–mouse IgG antibody was diluted 1:250 in blocking buffer solution and applied on a rocking plate for 5 to 7 days. Specimens were washed in PTX for 2 days, incubated in a solution containing streptavidin–biotinylated horseradish peroxidase for 2 days, washed again in PTX for 2 days, and then rinsed several times in 0.1 M Tris-HCl (pH 7.4); specimens were then exposed to 3,3′-diaminobenzidine and enhancement of staining with tap water. Fetuses were rinsed in distilled water followed by 2 washes in PBS, serially dehydrated in methanols, and then cleared and stored in methylsalicylate.

*Whole-Body Skeletal Preparation*

Fetuses obtained on embryonic Days 14.5 to 18.5 as well as postnatal Day 1 pups (80 specimens; three–10 of each phenotype at each age) were eviscerated and deskinned, then fixed in 4% PFA for several days. They were placed in Alcian blue solution for 6 days at 4˚C, rehydrated, transferred into alizarin red solution for 3 hours, and exposed to a series of glycerol-potassium-hydroxide solutions to clear the surrounding soft tissue before storage in 100% glycerol at room temperature.

## Results

Matings between doubly heterozygous males and homozygous curly tail females generated litters containing fetuses with three different phenotypes: lumbosacral spina

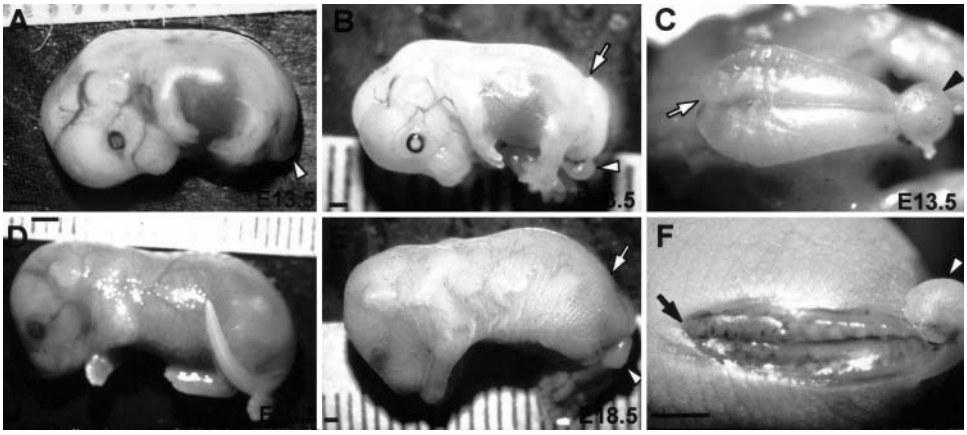


FIG. 1. Photographs showing the appearance of spina bifida in mouse fetuses. A–F: Fetuses with curly tail only (A), Spina bifida plus curly tail (B, C, E, and F) or normal tail/spine (D) at embryonic Day 13.5 (A–C) and embryonic Day 18.5 (D–F). *Arrowheads* indicate curled tails (A–C, E, and F), and *arrows* point to the cranial end of the open spina bifida lesion (B, C, E, and F). C and F: Magnified photographs showing posterior views of the fetuses in B and E, respectively. Note the bulging spina bifida lesion in B and C on embryonic Day 13.5 compared with the flattened degenerating lesion (E and F) on Day 18.5. Scale bars = 1 mm.

bifida of varying size combined with a curly tail (in 92 [34%] of 272 fetuses studied), curly tail alone (25.5%), and normal tail/spine (40.5%) (Fig. 1A–F).

*Abnormal Angulation of Spinal Nerve Roots in Fetuses With Spina Bifida*

Microdissection of the L6–S1 level in embryonic Day 18.5 normal fetuses showed spinal nerve roots running caudolaterally from the spinal cord toward the periphery (Fig. 2A). Conversely, in spina bifida littermates the direction of the spinal nerve roots was craniolateral from the spina bifida region of the spinal cord (Fig. 2B). To identify more clearly the microdissected posterior root ganglia with their respective sensory nerve roots, dissolved DiI crystals were injected into L6–S1 posterior root ganglia.

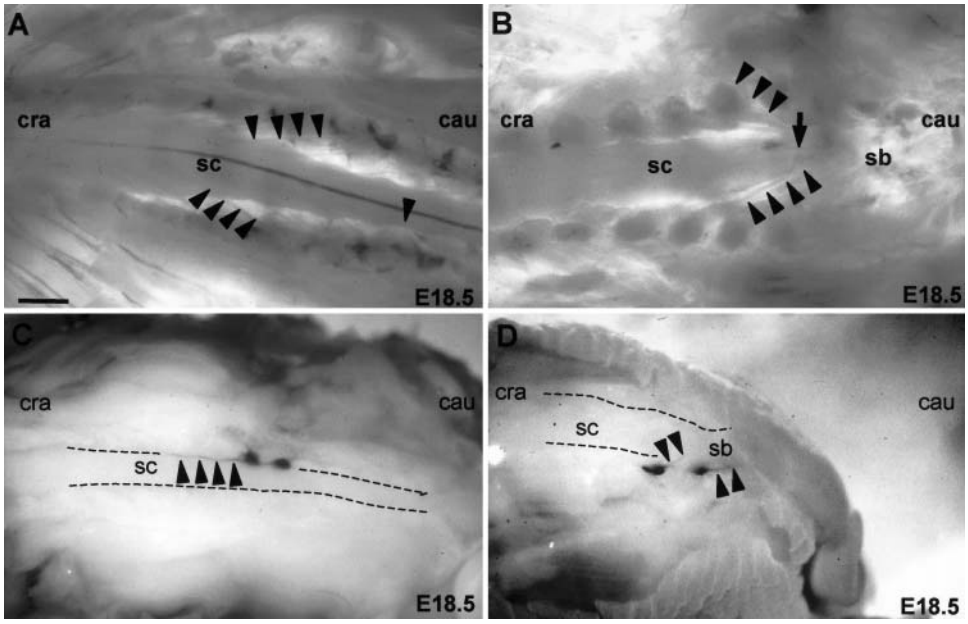


FIG. 2. Abnormal angulation of spinal nerve roots in whole-mount spina bifida fetuses. A and B: Posterior view of microdissected gestational Day 18.5 normal (A) and spina bifida (B) fetal specimens. Cranial is to the left and caudal is to the right. The *arrow* in B indicates the cranial end of the spina bifida lesion. *Arrowheads* trace the course of individual spinal nerve roots running from the spinal cord to the periphery. C and D: Posterior root ganglia labeled with DiI (L6–S1) and their respective sensory nerve roots *(arrowheads)* observed in embryonic Day 18.5 fetuses; posterior view of right-sided ganglia in a normal fetus (C) and posterolateral view of left-sided ganglia in a spina bifida fetus (D). *Dashed lines* indicate the edges of the spinal cord. cau = caudal; cra = cranial; sb = spina bifida; sc = spinal cord. Scale bars = 240 μm (A and B), and 400 μm (C and D).

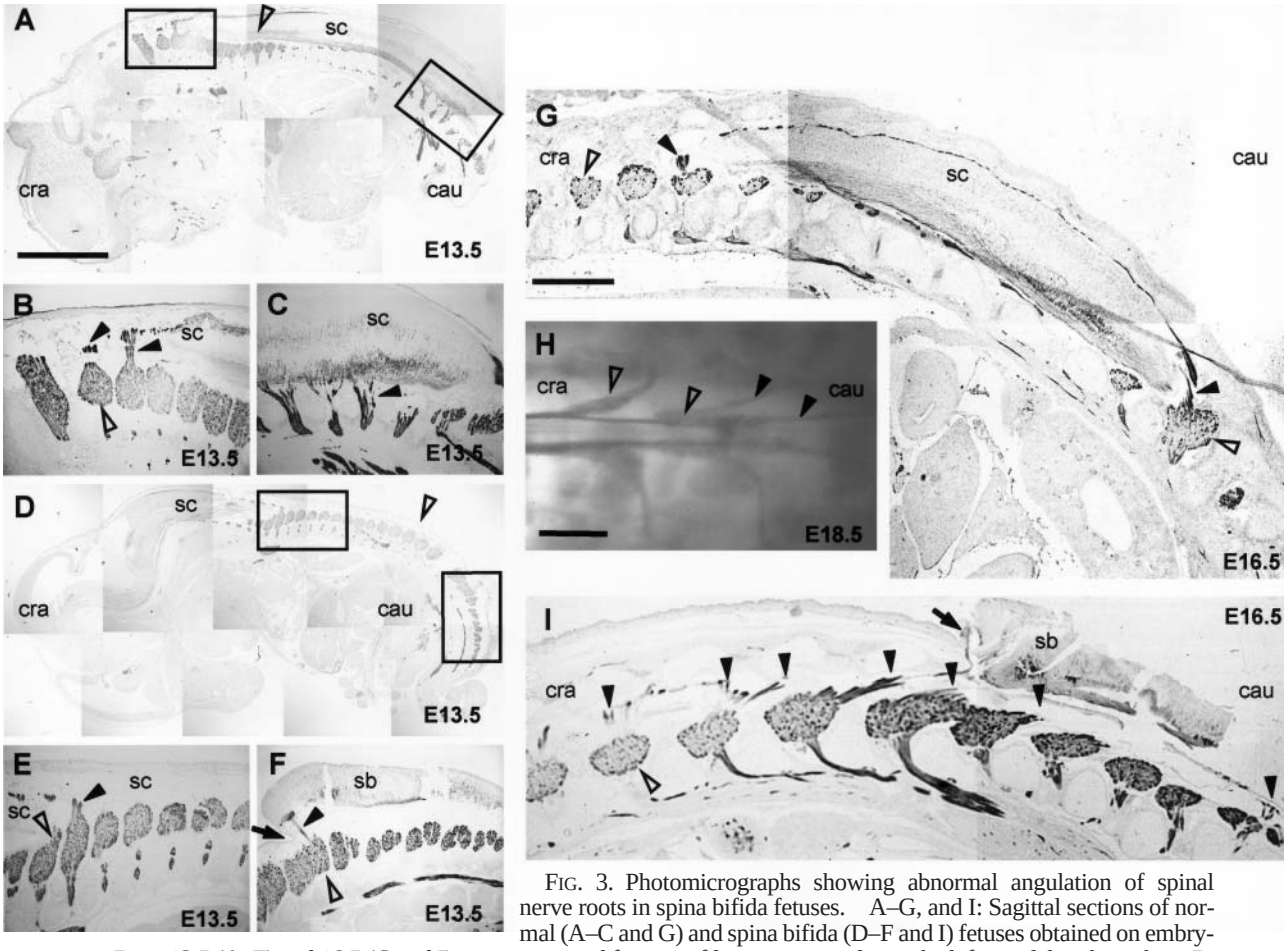


FIG. 3. Photomicrographs showing abnormal angulation of spinal nerve roots in spina bifida fetuses. A–G, and I: Sagittal sections of normal (A–C and G) and spina bifida (D–F and I) fetuses obtained on embryonic Days 13.5 (A–F) and 16.5 (G and I) immunostained for neurofilaments; cranial is to the left, caudal to the right. B, C, E, and F are magnifications of boxed areas in A and D, respectively. *Open arrowheads* mark the posterior root ganglia and *closed arrowheads* indicate the spinal nerve roots. The *closed arrows* in F and I indicate the cranial end of the spina bifida lesion. H: Whole-mount neurofilament immunostaining of a normal embryonic Day 18.5 fetus showing a posterior view of the conus medullaris with the terminal filum and the posterior root ganglia *(open arrowheads)*. Note the caudolateral direction of the nerve roots *(closed arrowheads)* leaving the spinal cord. Scale bars = 200 μm (A and D), 500 μm (B, C, E, and F), 475 μm (G and I), and 455 μm (H).

After several weeks' incubation, normal embryonic Day 18.5 fetuses showed sensory nerve roots running caudolaterally from the spinal cord at the L2–3 intervertebral space to the L6–S1 posterior root ganglia, indicating a physiological ascent of the spinal cord of three to four vertebrae (Fig. 2C). In contrast, in littermates with a large spina bifida lesion, the L6–S1 nerve roots ran craniolaterally from the spinal cord. This effect was most pronounced at the cranial end of the spina bifida lesion (Fig. 2D).

*Changing Angulation of Spinal Nerves With Progressive Gestation*

To assess the time course of spinal cord ascent, fetuses were processed for neurofilament immunostaining. Sections obtained in both normal and spina bifida fetuses at embryonic Days 12.5 to 14.5 showed spinal nerve roots running perpendicularly from the spinal cord to the periphery at all levels (Fig. 3A–F). After 14.5 days' gestation, the angle changed to an oblique one, but the angle of the nerve roots was in opposite directions in control and spina bifida animals. Normal fetuses showed a caudolateral direction of nerve roots from the spinal cord (pine tree–shaped pattern; Fig. 3G and H), whereas spina bifida fetuses exhibited a craniolateral direction of nerve roots from the spinal cord (V-shaped pattern), an effect that was most pronounced at the cranial end of the spina bifida lesion (Fig. 3I). Evaluation of whole-mount neurofilament preparations confirmed that the conus medullaris and the terminal filum of normal fetuses are well distinguished from each other, reaching S3–4 in normal fetuses by embryonic Day 18.5 (Fig. 3H). Whole-mount neurofilament staining of embryonic Day 18.5 fetuses with spina bifida did not yield clear results because of the degenerative changes occurring in the spina bifida lesion by this gestational stage (data not shown).

*Thinning of the Closed Spinal Cord in Spina Bifida Mice*

To determine whether tethering of spina bifida also affects other parts of the spinal cord, fetuses were processed for histological analysis. On embryonic Day 13.5, sagittal

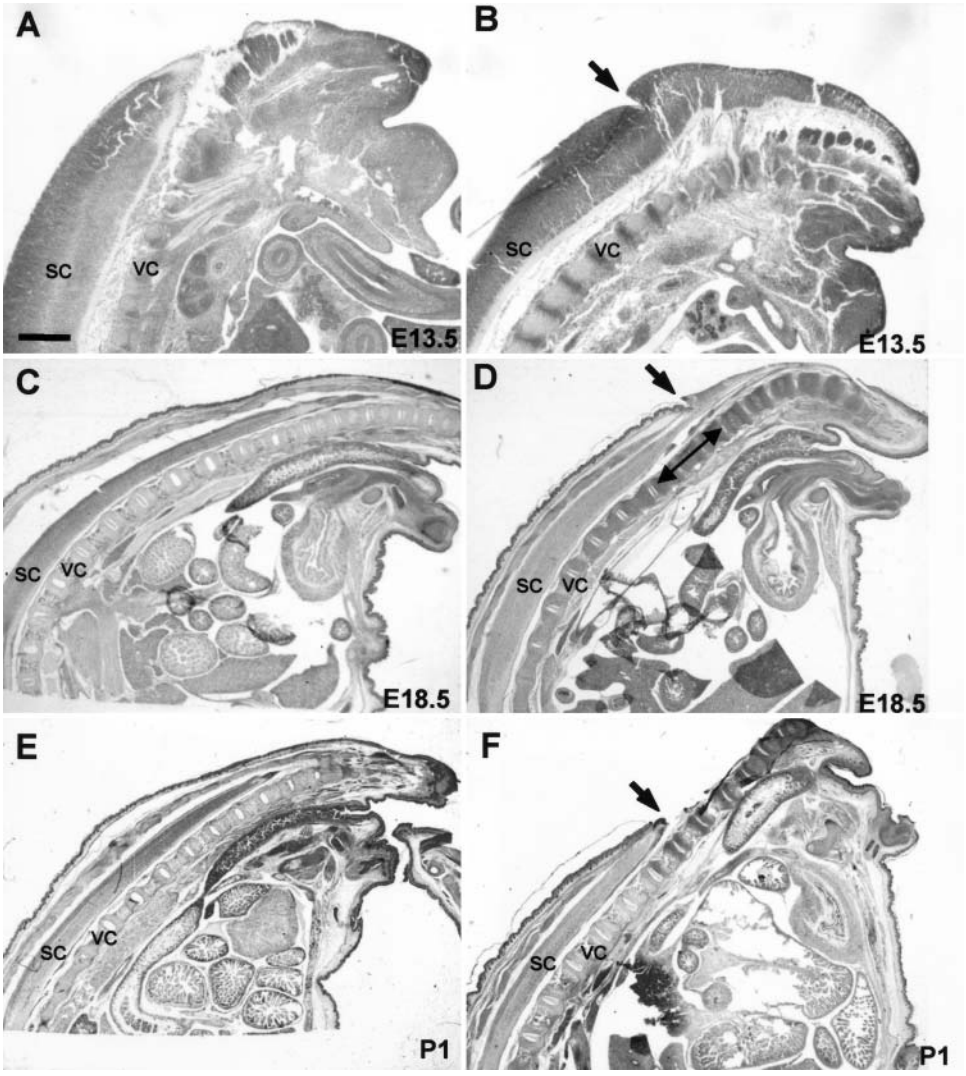


FIG. 4. Photomicrographs showing stretching of the closed spinal cord immediately cranial to the spina bifida lesion. Hematoxylin and eosin–stained sagittal sections obtained in normal (A, C, and E) and spina bifida (B, D, and F) fetuses on gestational Days 13.5 (A and B), and 18.5 (C and D) as well as neonates on postpartum Day 1 (E and F). The end of the tail is to the right. *Arrows* indicate the cranial end of the spina bifida lesion (B, D, and F). *Double-headed arrow* in D indicates the region of spinal cord narrowing just cranial to spina bifida lesion. vc = vertebral column. Scale bars = 4.2 mm (A and B), and 1 mm (C–F).

sections of spina bifida specimens showed an intact closed region of spinal cord, cranial to the spina bifida lesion, which had the same diameter as in normal littermates (Fig. 4A and B). By Day 16.5, however, the distal end of the closed spinal cord in spina bifida mice exhibited a slightly tapered appearance (data not shown), and as gestation progressed, this tapering became increasingly marked so that, by Day 18.5, the spinal cord region cranial to the spina bifida appeared markedly attenuated (Fig. 4C and D). On postnatal Day 1, however, this tapering was no longer visible because the spina bifida lesion had completely degenerated, releasing its tethering effect (Fig. 4E and F).

*Skeletal Lordosis and Kyphosis Before and After Spinal Cord Ascent*

In humans, the presence of a tethered cord can be associated with exacerbation of scoliosis. Whole-mount skeletal preparations on gestational Day 14.5, 1 day before the onset of the spinal cord ascent, showed an even curvature of the spine in normal fetuses. In contrast, in all spina bifida littermates, lordotic and kyphotic changes were observed in the region of the lower back (site of the spina bifida lesion) and the tail (data not shown). At all stages through postnatal Day 1, normal fetuses maintained an even curvature of the spine, whereas skeletal alterations were observed in the vertebral column in animals with spina bifida. This usually presented as a cranial lordosis followed by a distal kyphosis (Fig. 5). Scoliotic changes did not occur.

*Postnatal Consequences of Spina Bifida*

Although not the main focus of the study, it was noted

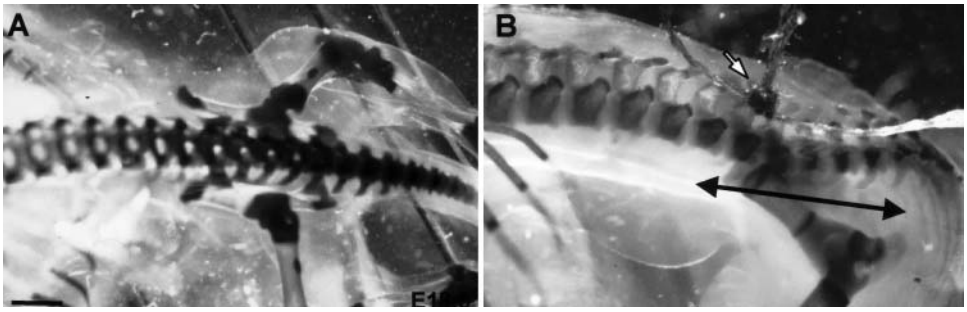


FIG. 5. Photographs showing kypholordotic deformity of the vertebral column in spina bifida fetuses. Skeletal preparations of the lumbar spinal region in a posterolateral view of mouse fetuses obtained in embryonic Day 18.5. Cranial is to the left, caudal to the right. Bone and cartilage are both stained. Note the even curvature of the spine in a normal fetus (A) compared with the kypholordotic spinal deformity in a spina bifida fetus (B). *Doubleheaded arrow* marks the region of the spina bifida lesion, the cranial end of which has been marked with a single suture *(white arrow)*. Scale bar = 480 μm.

that mice with spina bifida invariably progressed to birth, but rarely survived beyond the neonatal period. Their deaths resulted from hemorrhage at the lesion site, with consequent severe anemia and weakness that compromised their ability to compete with healthy littermates for maternal care and nutrition. Lower-extremity paralysis and loss of sensation were documented in some pups with large spina bifida lesions (D. Stiefel, unpublished data). Hence, although mice with spina bifida in the present model do not generally survive beyond the neonatal period, they do exhibit many of the features of human newborns with spina bifida.

## Discussion

In human embryos, closure of the neural tube in the spinal region is completed around gestational Day 30.[9] By Day 45 the spinal cord still shows the same length as its surrounding vertebral column, leading to a perpendicular course of the spinal nerve roots leaving the spinal cord. Thereafter, the very terminal end of the spinal cord undergoes morphogenetic changes, by which the fibrous terminal filum forms by approximately Day 54.[9] This process leads to an indirect ascent of the conus medullaris within the vertebral column to S-5,[13] but without changing the perpendicular angulation of the spinal nerve roots.[9] Beyond this time point, the ascent of the conus medullaris is attributed to true differences in growth rates between the spinal cord and the surrounding vertebrae, thus leading to an increasingly oblique (caudolateral) course of the nerve roots as they pass from the spinal cord to the intervertebral foramina.[9] Between Weeks 12 and 24 to 25, the level of the conus medullaris shows significant variation in individuals,[13] but by 24 weeks' gestation, it usually lies at S-1[9] or above S-1.[13] At birth the conus medullaris has reached L2–3[9] or L-3[13] and by 1 to 3 months postpartum the adult level of L1–2[9] or L2–3[13] intervertebral space is reached.

In contrast to the well-documented physiological ascent of the spinal cord in human fetuses, the spinal cord ascent in individuals with myelomeningocele is poorly understood, having been described in relatively few studies. In an investigation of dysraphic fetuses, Barson[2] showed that, beyond the gestational age of 9 weeks, spinal nerve roots within closed segments of the spinal cord become progressively angulated in a caudolateral direction, whereas nerve roots immediately cranial to the myelocele pass in a craniolateral fashion to the intervertebral foramina. Surprisingly, the same phenomenon was observed in cases of cervical myelomeningocele in which obliquely running nerves are unexpected, even in the case of the physiological ascent of the spinal cord. Fetuses in this study showed an additional Arnold Chiari Type II malformation, which might have been the cause of spinal nerve traction, of their changing angulation.

A tethered cord is a well-known complication in human dysraphism. It may be caused by various conditions such as thickened terminal filum, lipoma, dermoid, or myelo-(meningo)cele.[3,14,16,22,25,30] The latter, following postnatal surgical closure, is by far the most frequent origin,[5,18] with tethering reportedly occurring in 100,[3,4] 95,[5] or 78%[33] of cases. Considering this high incidence, it is surprising that only a low incidence of symptomatic tethering has been reported. Selber and Dias[26] cited a 29% rate of TCS in adults, whereas in children symptomatic tethering has been reported to occur in 38%,[5] more than 27,[19] 19,[3] 15,[30] and even 0%[4] of cases involving myelomeningocele.

The tethered cord, seen in individuals with myelomeningocele after postnatal closure, is usually a secondary effect of scar tissue formation at the operative site.[1,3,14,21,30] In contrast, cord tethering may be a primary finding in individuals with spina bifida occulta, where the latter is often only diagnosed following the onset of symptoms of tethering.[17,29] There is only one report of spinal cord tethering occurring prior to repair of a postnatal myelomeningocele,[33] similar to the findings in our mouse model. The absence of such reports may be attributed to the fact that the tethered cord is not a clinical feature commonly examined in newborns with myelomeningocele, because its diagnosis does not change the therapeutic approach, nor the indication for surgery.

In the present study of a mouse model, we found that ascent of the spinal cord during gestation begins by Day 15.5 in both normal and spina bifida fetuses. Prior to this day, the nerve roots run perpendicular to the spinal cord, whereas later in gestation they run obliquely from the spinal cord (Fig. 6). Strikingly, however, normal fetuses exhibit nerve roots running caudolaterally from the spinal cord, whereas fetuses with spina bifida exhibit craniolaterally running nerves. Thus, spina bifida appears to prevent the physiological ascent of the spinal cord due to

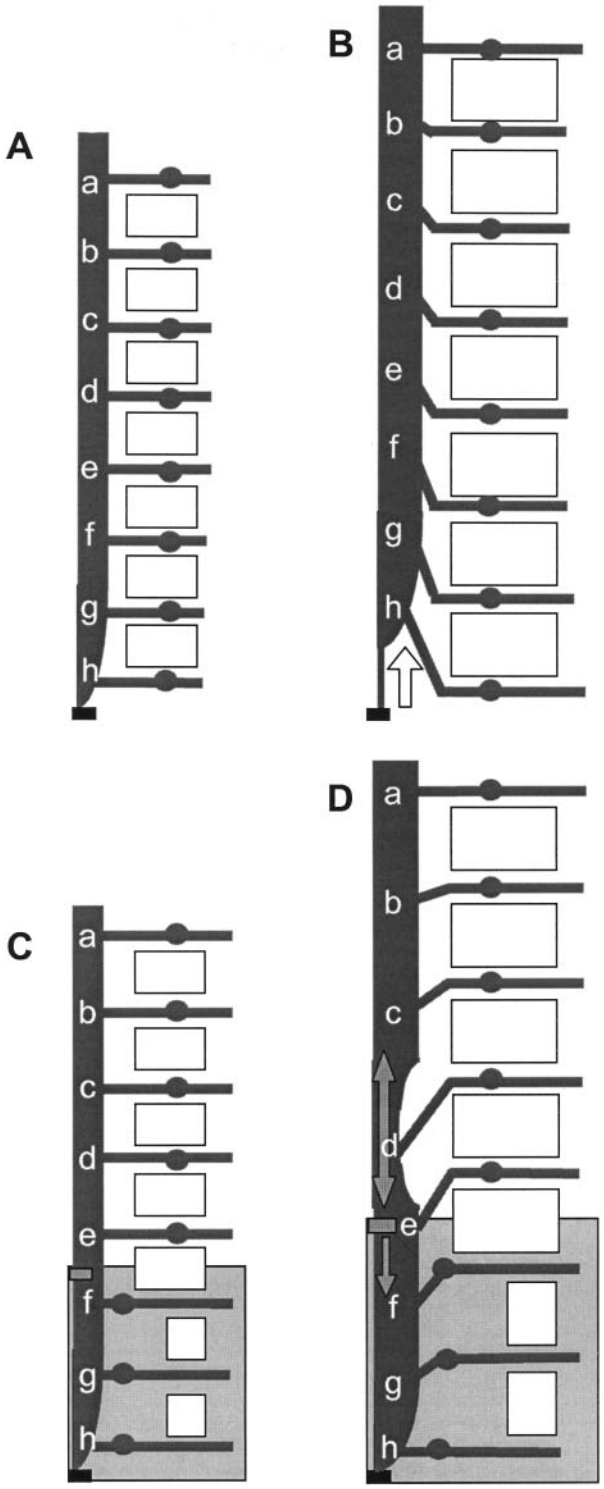


pathological fixation of the primary malformed spina bifida to the surrounding tissue, leading to the appearance of a tethered cord. Furthermore, we found that cord tethering affects the morphology of the portion of closed spinal cord immediately proximal to the spina bifida lesion, which progressively elongates and tapers, apparently as a compensatory stretching mechanism. As a result of this localized cord elongation, nerve roots cranial to the lesion become gradually less obliquely angled (Fig. 6).

Overextension of the spinal cord may cause axonal damage directly as well as indirectly decreasing oxygenation of the neural tissue due to ischemia and metabolic deficiency. Both effects could contribute to the atrophy and decrease in diameter observed in the distal part of the closed spinal cord in our study. A similar finding of an atrophic spinal cord was reported in 44% of individuals with TCS.[4] In a few studies investigators have produced experimental spinal cord traction to simulate the TCS,[8,10,11,31,34] and all authors concluded that spinal cord traction produces metabolic dysfunction and ischemia.

If metabolic deficiency and ischemia are indeed elicited by a tethered overstretched spinal cord, then progressive neuronal injury is likely[34] to occur in conjunction with progressive sensorimotor deficit, as often observed in humans with tethered cord.[5,14,24,25,30,32] Examination of the mouse model also showed a neurological deficit developing in late gestation, in which the level of the deficit correlated closely with the size of the open spina bifida (D. Stiefel, unpublished data). This neurological deficit, however, does not involve more proximally located spinal nerves, perhaps because tethering in the mouse is only of short duration (embryonic Days 15.5–18.5), in contrast to the long-term nature of TCS in humans, with its progressive development of sensorimotor deficit. Alternatively, the assessment techniques to detect neurological deficit in mouse fetuses may be too insensitive to detect partial sensorimotor weakness or numbness, findings that are typical in cases of progressive TCS.

Other mechanisms that may lead to overstretched tethered nerve roots could include abnormal curvature of the spine. Our animal model of spina bifida shows various grades of kyphosis and lordosis throughout gestation, defects that originate as early as embryonic Day 13.5 or 14.5, prior to the onset of the spinal cord ascent. This would argue that the abnormal spinal curvature is unlikely to cause the progressive tethering but is more likely a result of progressive cord tethering, as often described in humans.[5,19,21,23–26]

FIG. 6. Depiction of spinal cord ascent in normal (A and B) and spina bifida (C and D) fetal mice with increasing gestation. The anatomy is depicted before (A and C) and after (B and D) the onset of spinal cord ascent. Cranial is to the top, caudal to the bottom. Each letter (a–h) marks the origin of a spinal nerve root running from the spinal cord. *Open rectangles* symbolize vertebrae (with only vestigial stumps in the region of the spina bifida), *large shaded rectangles* in C and D indicate the region of open spina bifida lesion and *small shaded rectangles* in C and D show the point of spinal cord tethering. The *open arrow* in B shows the direction of the physiological ascent of the spinal cord in normal fetuses, whereas the *single-headed gray arrow* in D shows the direction of the tethering force. The *double-headed gray arrow* in D shows the resulting stretching of the untethered closed spinal cord region immediately cranial to the spina bifida. Note that the angulation of spinal nerves is caudolateral from spinal cord to ganglia in the normal fetus (B) but craniolateral in the spina bifida fetus (D).

## Conclusions

Our finding of spinal cord tethering in an experimentally tractable mouse model of spina bifida provides further insight into the clinically important phenomenon of spinal cord tethering and its early sequelae. Potential future studies involving this mouse model will include determining the time course of neural degeneration in the exposed spina bifida lesion, the contribution of tethering-induced stretch compared with exposure to amniotic fluid in the pathogenesis of neural degeneration, and the relative onset of ischemia, metabolic dysfunction, and axonal/neuronal injury in the tethered cord. The contribution of spinal cord tethering to the pathogenesis of hindbrain herniation and hydrocephalus is also an area for future study. Preliminary results derived from fetal surgery in human spina bifida have demonstrated a lower incidence of hydrocephalus postnatally, suggesting that untethering of the spina bifida lesion may contribute to minimization of hindbrain herniation.[7,28] It will be instructive to determine the relationship between cord tethering and hindbrain herniation in the mouse spina bifida model.

### Acknowledgment

We thank Dr. Saadi Ghatan for valuable comments on this manuscript.

### References

1. Banta JV: The tethered cord in myelomeningocele: should it be untethered? **Dev Med Child Neurol 33:**173–176, 1991
2. Barson AJ: Spina bifida: the significance of the level and extent of the defect to the morphogenesis. **Dev Med Child Neurol 12:**129–144, 1970
3. Begeer JH, Meihuizen de Regt MJ, HogenEsch I, et al: Progressive neurological deficit in children with spina bifida aperta. **Z Kinderchir 41:**S13–S15, 1986
4. Bono R, Inverno M, Botteon G, et al: Clinical features and MR imaging in children with repaired myelomeningocele. **Ital J Neurol Sci 14:**553–559, 1993
5. Brezner A, Kay B: Spinal cord ultrasonography in children with myelomeningocele. **Dev Med Child Neurol 41:**450–455, 1999
6. Bruce DA, Schut L: Spinal lipomas in infancy and childhood. **Childs Brain 5:**192–203, 1979
7. Bruner JP, Tulipan N, Paschall RL, et al: Fetal surgery for myelomeningocele and the incidence of shunt-dependent hydrocephalus. **JAMA 282:**1819–1825, 1999
8. Cusick JF, Myklebust J, Zyvoloski M, et al: Effects of vertebral column distraction in the monkey. **J Neurosurg 57:**651–659, 1982
9. Dias MS: Myelomeningocele, in Choux M, Di Rocco C, Hockley AD, et al (eds): **Pediatric Neurosurgery.** New York: Churchill Livingstone, 1999, pp 33–59
10. Dolan EJ, Transfeldt EE, Tator CH, et al: The effect of spinal distraction on regional spinal cord blood flow in cats. **J Neurosurg 53:**756–764, 1980
11. Fujita Y, Yamamoto H: An experimental study on spinal cord traction effect. **Spine 14:**698–705, 1989
12. Gruneberg H: Genetical studies on the skeleton of the mouse. VIII. Curly tail. **J Genet 52:**52–67, 1954
13. Hawass ND, el-Badawi MG, Fatani JA, et al: Myelographic study of the spinal cord ascent during fetal development. **AJNR Am J Neuroradiol 8:**691–695, 1987
14. Herman JM, McLone DG, Storrs BB, et al: Analysis of 153 patients with myelomeningocele or spinal lipoma reoperated upon for a tethered cord. Presentation, management and outcome. **Pediatr Neurosurg 19:**243–249, 1993
15. Hoffman HJ, Hendrick EB, Humphreys RP: The tethered spinal cord: its protean manifestations, diagnosis and surgical correction. **Childs Brain 2:**145–155, 1976
16. Hoffman HJ, Taecholarn C, Hendrick EB, et al: Management of lipomyelomeningoceles. Experience at the Hospital for Sick Children, Toronto. **J Neurosurg 62:**1–8, 1985
17. Mapstone TB: Management of tethered spinal cord. **Neurosurg Q 4:**82–91, 1994
18. McLone DG: The adult with a tethered cord. **Clin Neurosurg 43:**203–209, 1996
19. McLone DG: Continuing concepts in the management of spina bifida. **Pediatr Neurosurg 18:**254–256, 1992
20. McLone DG: Occult dysraphism and the tethered spinal cord, in Choux M, DiRocco C, Hockley AD, et al (eds): **Pediatric Neurosurgery.** New York: Churchill Livingstone, 1999, pp 61–100
21. McLone DG, Herman JM, Gabrieli AP, et al: Tethered cord as a cause of scoliosis in children with a myelomeningocele. **Pediatr Neurosurg 16:**8–13, 1990
22. McLone DG, Naidich TP: Laser resection of fifty spinal lipomas. **Neurosurgery 18:**611–615, 1986
23. Pierz K, Banta J, Thomson J, et al: The effect of tethered cord release on scoliosis in myelomeningocele. **J Pediatr Orthop 20:**362–365, 2000
24. Reigel DH, Tchernoukha K, Bazmi B, et al: Change in spinal curvature following release of tethered spinal cord associated with spina bifida. **Pediatr Neurosurg 20:**30–42, 1994
25. Sarwark JF, Weber DT, Gabrieli AP, et al: Tethered cord syndrome in low motor level children with myelomeningocele. **Pediatr Neurosurg 25:**295–301, 1996
26. Selber P, Dias L: Sacral-level myelomeningocele: long-term outcome in adults. **J Pediatr Orthop 18:**423–427, 1998
27. Strong LC, Hollander WF: Hereditary loop-tail in the house mouse. **J Hered 40:**329–334, 1949
28. Sutton LN, Adzick NS, Bilaniuk LT, et al: Improvement in hindbrain herniation demonstrated by serial fetal magnetic resonance imaging following fetal surgery for myelomeningocele. **JAMA 282:**1826–1831, 1999
29. Tadmor R, Ravid M, Findler G, et al: Importance of early radiologic diagnosis of congenital anomalies of the spine. **Surg Neurol 23:**493–501, 1985
30. Tamaki N, Shirataki K, Kojima N, et al: Tethered cord syndrome of delayed onset following repair of myelomeningocele. **J Neurosurg 69:**393–398, 1988
31. Tani S, Yamada S, Knighton RS: Extensibility of the lumbar and sacral cord. Pathophysiology of the tethered spinal cord in cats. **J Neurosurg 66:**116–123, 1987
32. Vernet O, O'Gorman AM, Farmer JP, et al: Use of the prone position in the MRI evaluation of spinal cord retethering. **Pediatr Neurosurg 25:**286–294, 1996
33. Vogl D, Ring-Mrozik E, Baierl P, et al: Magnetic resonance imaging in children suffering from spina bifida. **Z Kinderchir 42:**S60–S64, 1987
34. Yamada S, Zinke DE, Sanders D: Pathophysiology of "tethered cord syndrome." **J Neurosurg 54:**494–503, 1981

Manuscript received November 5, 2002.
Accepted in final form May 27, 2003.
Dr. Stiefel received funding from the University of Zurich, Switzerland, Research Fellowship and Dr. Copp received a Programme Grant (no. 051690) from the Wellcome Trust, United Kingdom.

*Address reprint requests to:* Andrew Copp, M.D., Ph.D., Neural Development Unit, Institute of Child Health, University College London, 30 Guilford Street, London WC1N 1EH, United Kingdom. email: a.copp@ich.ucl.ac.uk.